ChemComm

COMMUNICATION

View Article Online
View Journal | View Issue

Cite this: *Chem. Commun.*, 2025, **61**, 8552

Received 28th January 2025,
Accepted 23rd April 2025

DOI: 10.1039/d5cc00527b

rsc.li/chemcomm

Comparative analysis of sulfated L-idose and L-iduronic acid in neoproteoglycan cell surface engineering†

Rakesh Raigawali, ‡[a] Saurabh Anand,‡[a] Ankita Chandra,[a] Virendrasinh Mahida,[a] Preeti Ravindra Bhoge,[a] Jancy Nixon Abraham[a] and Raghavendra Kikkeri *[ab]

Herein, we report the synthesis of heparan sulfate (HS) proteoglycan mimetics bearing iduronic acid (IdoA) and sulfated L-idose (Ido) hexasaccharides to assess how these isostructural sugars with similar charge density influence neoproteoglycan display on the cell membrane. PG@I2, carrying sulfated L-idose, showed rapid internalization in both cancerous and normal cells, whereas PG@I1, containing native IdoA expressed on the cell membrane and slowly internalized, underscoring the role of IdoA in HSPG cell surface engineering.

Heparan sulfate (HS) is a polysulfated glycosaminoglycan (GAG) widely present on cell surfaces and within the extracellular matrix. HS engages in interactions with a multitude of proteins, including growth factors, chemokines, and enzymes, playing a pivotal role in signaling pathways critical to cellular growth, differentiation, immune responses, and angiogenesis.[1] Structurally, HS consists of repeating disaccharide units composed of D-glucuronic acid (GlcA) or its epimer L-iduronic acid (IdoA), linked to glucosamine (GlcN) residues.[2] These units exhibit diverse sulfation patterns and acetylation. The conformational flexibility of IdoA, particularly its ability to adopt multiple forms such as the chair ($^1C_4$), skew-boat ($^2S_0$), and boat conformations, enables specific and dynamic interactions with proteins.[3] This structural diversity endows HS with exceptional functional versatility and specificity in biological recognition processes. Consequently, there is considerable research interest in understanding the specific roles of each component of HS in detail. Among these, L-iduronic acid is particularly intriguing due to its synthetic challenges and conformational flexibility.[4] Previously, L-iduronic acid in the anticoagulant drug fondaparinux and idraparinux was substituted with isostructural sugars, including D-glucuronic acid, D-xylose and 6-deoxy-L-talose moiety respectively. These substitutions resulted in the loss of anticoagulant activity, emphasizing the critical importance of L-iduronic acid in the anticoagulation activity of the drugs.[5,6] To elucidate the importance of the specific conformation of L-iduronic acid in anticoagulation activity, $^1C_4$ and $^2S_0$ conformation of L-iduronic acid were locked in idraparinux and their anticoagulation activities were compared.[7] These studies underscore the crucial importance of the $^2S_0$ conformational of L-iduronic acid in idraparinux for its anticoagulant function. Recently, we reported the synthesis of sulfated homo-oligo L-iduronic acid and elucidated the significance of the trisaccharide as the minimal binding motif required for FGF2 recognition.[4] Another significant characteristic of HS is its anionic sulfate-carboxylate composition, which plays a key role in biological recognition. However, the rationale behind nature's selection of such anionic combination remains unclear, as does the potential impact of fully sulfated HS. To explore this question, herein, we synthesized two hexasaccharides: one incorporating the native L-iduronic acid ligand and the other containing sulfated L-idose as the uronic acid residue and conjugated

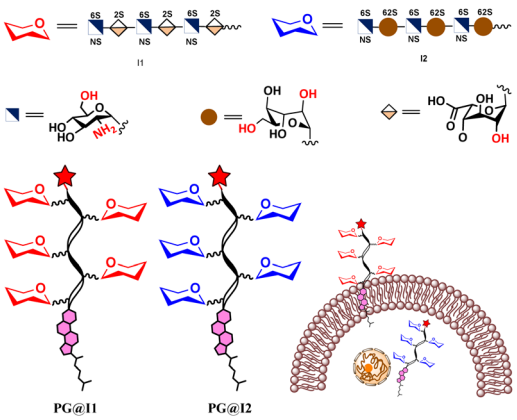

Fig. 1 Schematic representation of neoproteoglycans and its cell surface engineering.

[a] *Indian Institute of Science Education and Research, Pune 411008, India*
[b] *Department of CPAS, Jackson State University, Jackson 39217, USA.*
E-mail: rkikkeri@iiserpune.ac.in; Fax: +91-20-25908207; Tel: +91-20-25908207

† Electronic supplementary information (ESI) available. See DOI: https://doi.org/10.1039/d5cc00527b

‡ Equal contribution.

onto a neoproteoglycan backbone to investigate their role in cell surface engineering.[8] Despite both molecules possessing 12 anionic groups, they are expected to exhibit distinct cell surface arrangement and internalization behaviors. These findings highlight the critical importance of the L-iduronic acid of HSPGs cell surface engineering (Fig. 1).

We synthesized sulfated L-idose and L-iduronic acid HS hexasaccharides using a [4+2] glycosylation strategy involving donor **1** and acceptor **2**, both prepared according to previously reported procedures.[9] The glycosylation of **1** and **2**, in the presence of *N*-iodosuccinimide (NIS) and trimethylsilyl trifluoromethanesulfonate (TMSOTf) as a promoter, resulted in hexasaccharide **3**. This intermediate underwent acetolysis using acetic anhydride and copper(II) trifluoromethanesulfonate as a catalyst. Subsequent treatment with phenyl trimethylsilyl sulfide and ZnI_2 generated the corresponding thioglycoside donor **5**. Further, linker glycosylation was performed, followed by selective deprotection of TBDPS groups using a hydrogen fluoride: pyridine complex in pyridine. Deacetylation and debenzoylation using a lithium hydroxide solution, along with *O*-sulfation in the presence of $SO_3{\cdot}Et_3N$ in DMF, yielded the sulfated L-idose hexasaccharide precursor **9** (Scheme 1). The C-2 azide group of **9** was then reduced to an amine using trimethylphosphine, resulting in compound **10**. *N*-Sulfation of the amine was achieved using the $SO_3{\cdot}$pyridine

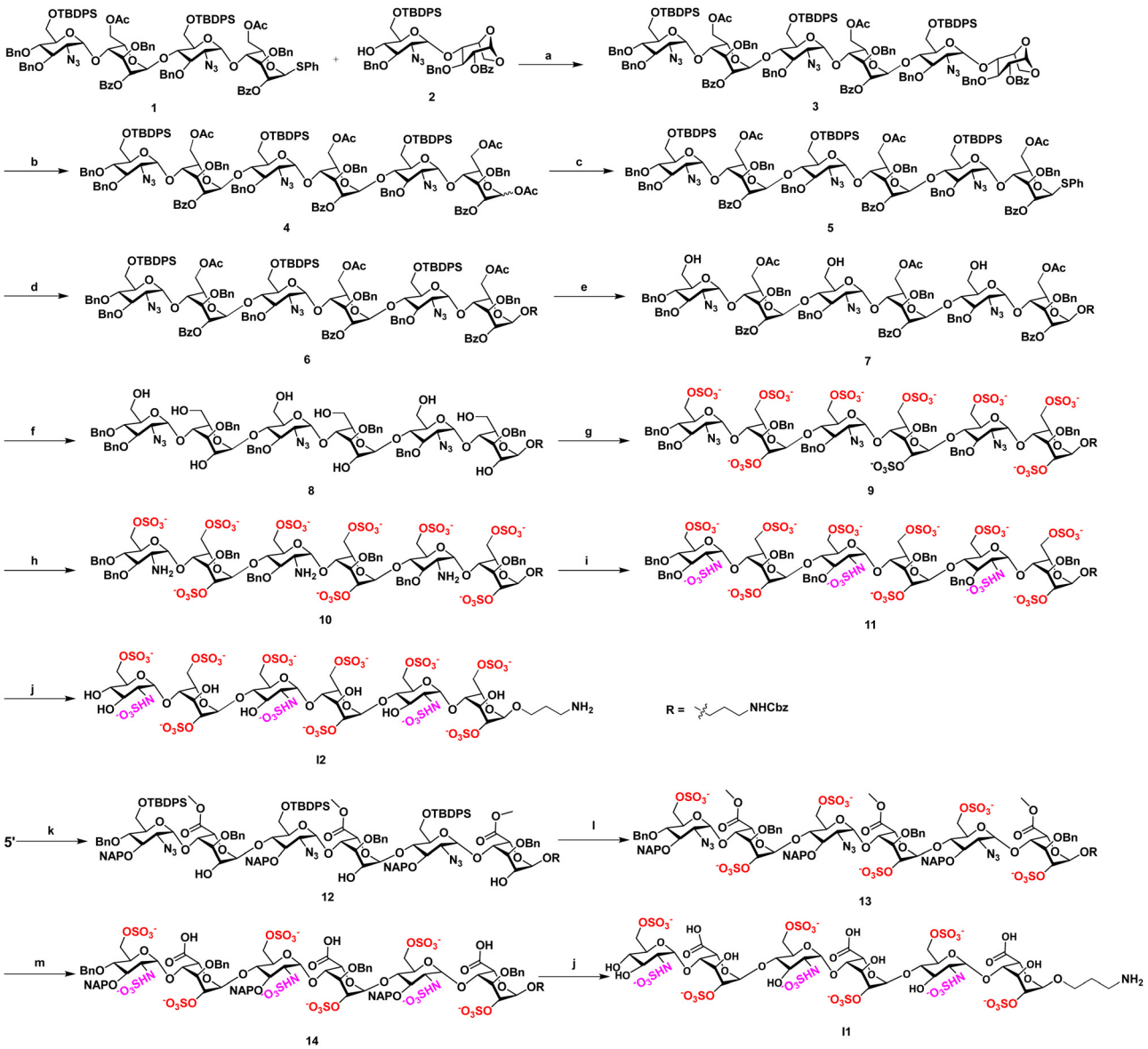

Scheme 1 Synthesis of **I2** and **I1** hexasaccharides: (a) NIS, TMSOTf, 4 Å MS −10 °C, DCM, 30 min; (b) Ac_2O, $Cu(OTf)_2$, rt, 12 h; (c) TMSSPh, ZnI_2, DCM, rt, 2 h; (d) benzyl (3-hydroxypropyl)carbamate, NIS, TMSOTf, 4 Å MS, 0 °C, DCM, 10 min; (e) HF. Py, Py, 0 °C, 12 h; (f) LiOH, H_2O : THF(1 : 1), rt, 12 h; (g) SO_3. NMe_3, DMF, MW, 100 °C, 30 min; (h) PMe_3. THF, THF, 1 N NaOH, rt, 12 h; (i) SO_3. Py. MeOH, 1N NaOH, 48 h; (j) H_2, $Pd(OH)_2$, H_2O, rt, 48 h; (k) (i) benzyl (3-hydroxypropyl)carbamate, NIS, TMSOTf, 4 Å MS, −10 °C, CH_2Cl_2; (ii) NaOMe, CH_2Cl_2/MeOH (1/1); (iii) TEMPO, CH_2Cl_2/MeOH (1/1); (iv) MeI, K_2CO_3, DMF; (v) LiOH. H_2O, H_2O/THF (1/1); (l) (i) HF. Py/Py 0 °C; (ii) SO_3. NMe_3, DMF, 60 °C; (m) (i) LiOH, MeOH; (ii) 1M PMe_3. THF, 0.1M $NaOH_{aq}$; (iii) SO_3. Py, MeOH.

complex. Finally, global deprotection through hydrogenolysis afforded the desired **I2**. Similarly, deacetylation of intermediate **5′**, followed by TEMPO-mediated oxidation and subsequent methyl esterification, yielded compound **12**. Compound **12** was further subjected to selective TBDPS deprotection, *O*-sulfation, reduction, *N*-sulfation, and global deprotection following the previously described procedures, yielded **I1**.[9] Both hexasaccharide were conjugated to DBCO linker and the crude DBCO conjugates were functionalized with a fluorescent amphiphilic peptide **PG@N3**, to obtain desired neoproteoglycans (neoPGs: **PG@I1** and **PG@I2**). NeoPGs were purified by HPLC using MeOH/H_2O as an eluent. The product purity and conjugation were confirmed from IR, HPLC and mass spectra of the complex.

To decode the role of L-idose and L-iduronic acid in the synthesized compounds **PG@I1** and **PG@I2** in cell surface engineering, MDA-MB-468 (aggressive breast cancer cell line), MCF-7 (mild breast cancer cells) and NIH-3T3 (normal fibroblast cell line) were used. A solution of neoPGs (2 μM) was incubated with the

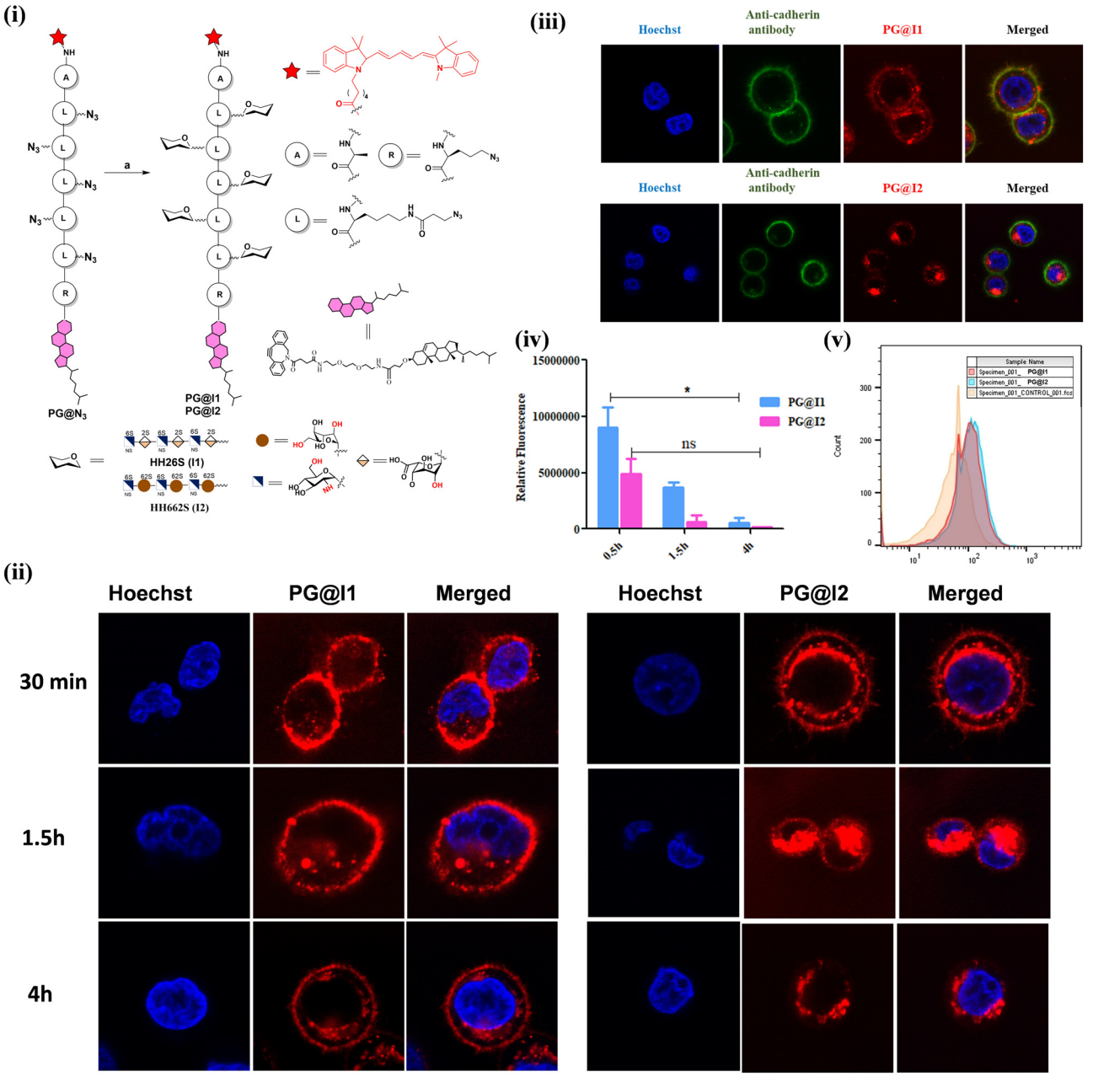

Fig. 2 (i) Synthesis of neoproteoglycan: (a) I1-DBCO or I2-DBCO in DMF at RT for 7 days; (ii) confocal images illustrating time-dependent uptake of proteoglycan mimic **PG@I1** and **PG@I2** (red fluorescent) DAPI (blue fluorescent) in MDA-MB-468 cell line (images taken at 100X); (iii) co-localization of **PG@I1/I2** (red) with anti-cadherin antibody (green) on the cell surface of MDA-MB-468 cells after 4 h; (iv) average fluorescence quantification of **PG@I1** and **PG@I2** on cell membrane of MDA-MB-468 cell line at different time intervals, n = 50 cells; (v) flow cytometric analysis of **PG@I1** and **PG@I2** uptake after 1.5 h incubation in MDA-MB 468 cells.

cells for 30 minutes, followed by washing to remove the excess neoPGs from the medium. For understanding the internalization of neoPGs in the cell line, time dependent confocal imaging was performed. Confocal images revealed significant differences in the plasma membrane (PM) expression and internalization of the neoPGs. In MDA-MB-468 cells, **PG@I2** demonstrated internalization within 30 minutes (Fig. 2(ii)), whereas **PG@I1** exhibited intense fluorescence on the PM and continued to localize there even after 4 hours. The flow cytometric measurement after 1.5 h showed similar amount of neoPGs internalization, indicating that the structural heterogeneity on neoPGs modulates the cell surface engineering process (Fig. 2(v)) This noteworthy difference in the colocalization process suggests that **PG@I1** is more effective in decorating the cell membrane compared to **PG@I2**. To confirm the decoration of the cell membrane and internalization of **PG@I1** and **PG@I2**, co-staining was performed using a green fluorescent anti-cadherin antibody (Fig. 2(iii)). Surprisingly even at 4 h of incubation of neoPGs there was a clear difference between **PG@I1** (Pearson coefficient: $p \sim 0.5$) and **PG@I2** ($p \sim 0.29$). A distinct coalescing of both green and red fluorescence on the cell membrane was observed for **PG@I1**, revealing a better ability of glycocalyx engineering. Interestingly, **PG@I1** exhibited slightly faster internalisation in MCF-7 and NIH-3T3 cells compared to MDA-MB-468. In contrast, **PG@I2** showed no evident cell surface decoration. These observations align with our previous findings,[8a] highlighting that variations in glycocalyx composition and surface receptors between normal, mild and triple negative breast cancer cells influence neoproteoglycan cell surface presentation.

This differential behaviour can be attributed to two key structural factors. Firstly, **PG@I2** exhibits a significantly higher negative charge than **PG@I1** at physiological pH, which enhances its interaction with positively charged domains on cell surface receptors. This stronger electrostatic attraction facilitates more efficient endocytosis. Given that NIH-3T3, MCF-7, and MDA-MB-468 cells possess distinct surface zeta potentials,[10] molecules with higher negative charge densities are internalized more rapidly than their less charged counterparts. Secondly, the native I1 is likely to interact with a broader spectrum of cell surface receptors and exhibits greater stabilisation on the cell membrane compared to I2. Overall, native heparan sulphate (HS) ligands appear to be crucial for the expression of neoPGs on the cell surface, whereas the highly sulphated PG@I2 primarily promotes endocytosis and may serve as a promising platform for cargo delivery applications.

In summary, we successfully synthesized HS hexasaccharides of L-iduronic acid (**I1**) and 6-*O*-sulfated L-idose residue (**I2**) using a [4+2] glycosylation strategy. These HS ligands were functionalized on amphiphilic glycopeptides through a copper-free click reaction. Cell surface engineering experiments revealed marked differences between the two molecules. **PG@I1** remained associated with the cell membrane for an extended period, while **PG@I2** was internalized within minutes. These findings highlight the critical role of the L-iduronic acid in the cell surface decoration of proteoglycans, whereas complete sulfation of HS ligands promotes endocytosis.[8a] We are currently exploring the potential cargo delivery applications of **PG@I2** and the glycocalyx remodeling capabilities of **PG@I1**.

This work is supported by IISER, Pune, DST (Grant No. SR/NM/NS-1113/2016), DBT (Grant No. BT/PR21934/NNT/28/1242/2017), P. R. B. acknowledges DST WOS-A grant SR/WOS-A/CS-72/2019 for financial support. All cells lines are procured from NCCS cell repository, Pune. India.

Data availability

The data supporting this article is provided in the ESI.†

Conflicts of interest

There are no conflicts to declare.

Notes and references

1 (*a*) I. Capila and R. J. Linhardt, *Angew. Chem., Int. Ed.*, 2002, **41**, 391–412; (*b*) J. R. Bishop, M. Schuksz and J. D. Esko, *Nature*, 2007, **446**, 1030–1037; (*c*) D. Xu and J. D. Esko, *Annu. Rev. Biochem.*, 2014, **83**, 129–157.
2 (*a*) C. Noti and P. H. Seeberger, *Chem. Biol.*, 2005, **12**, 731–756; (*b*) J. T. Gallagher and J. E. Turnbull, *Glycobiology*, 1992, **2**, 523–528; (*c*) D. Spillmann and U. Lindahl, *Curr. Opin. Struct. Biol.*, 1994, **4**, 677–682; (*d*) K. S. Rostand and J. D. Esko, *Infect. Immun.*, 1997, **65**, 1–8.
3 (*a*) J. Kreuger, D. Spillmann, J. P. Li and U. Lindahl, *J. Cell Biol.*, 2006, **174**, 323–327; (*b*) C. Noti and P. H. Seeberger, *Chem. Biol.*, 2005, **12**, 731–756; (*c*) J. C. Muñoz-García, J. López-Prados, J. Angulo, I. Díaz-Contreras, N. Reichardt, J. L. de Paz, M. Martín-Lomas and P. M. Nieto, *Chem. – Eur. J.*, 2012, **18**, 16319–16331.
4 C. D. Shanthamurthy, A. Gimeno, S. Leviatan Ben-Arye, N. V. Kumar, P. Jain, V. Padler-Karavani, J. Jiménez-Barbero and R. Kikkeri, *ACS Chem. Biol.*, 2021, **16**, 2481–2489.
5 C. A. A. Van Boeckel and M. Petitou, *Angew. Chem., Int. Ed. Engl.*, 1993, **32**, 1671–1690.
6 (*a*) F. Demeter, T. Demeter, Z. Bereczky, K. E. Kövér, M. Herczeg and A. Borbás, *Sci. Rep.*, 2018, **8**, 13736; (*b*) M. Herczeg, F. Demeter, E. Lisztes, M. Racskó, B. I. Tóth, I. Timári, Z. Bereczky, K. E. Kövér and A. Borbás, *J. Org. Chem.*, 2022, **87**, 15830–15836.
7 S. K. Das, J. M. Mallet, J. Esnault, P. A. Driguez, P. Duchaussoy, P. Sizun, J. P. Herault, J. Herbert, M. Petitou and P. Sinaÿ, *Chem. –Eur. J.*, 2001, **7**, 4821–4834.
8 (*a*) S. Anand, P. R. Bhoge, R. Raigwali, S. V. Saladi and R. Kikkeri, *Chem. Sci.*, 2024, **15**, 19962–19969; (*b*) S. Anand, S. Mardhekar, P. R. Bhoge, S. K. Mishra and R. Kikkeri, *Chem. Commun.*, 2024, **60**, 4495–4498.
9 (*a*) P. Jain, C. D. Shanthamurthy, P. M. Chaudhary and R. Kikkeri, *Chem. Sci.*, 2021, **12**, 4021–4027; (*b*) S. Mardhekar, B. Subramani, P. Samudra, P. Srikanth, V. Mahida, P. Ravindra Bhoge, S. Toraskar, N. M. Abraham and R. Kikkeri, *Chem. – Eur. J.*, 2023, **29**(7), e202202622; (*c*) S. Spijkers-Shaw, R. Devlin, N. J. Shields, X. Feng, T. Peck, G. Lenihan-Geels, C. Davis, S. L. Young, A. C. La Flamme and O. V. Zubkova, *Angew. Chem., Int. Ed.*, 2024, **63**, e20231691; (*d*) P. Chopra, T. Yadavalli, F. Palmieri, S. A. K. Jongkees, L. Unione, D. Shukla and G. J. Boons, *Angew. Chem., Int. Ed.*, 2023, **62**, e202309838; (*e*) Y. P. Hu, Y. Q. Zhong, Z. G. Chen, C. Y. Chen, Z. Shi, M. M. Zulueta, C. C. Ku, P. Y. Lee, C. C. Wang and S. C. Hung, *J. Am. Chem. Soc.*, 2012, **134**, 20722–20727; (*f*) K. N. Baryal, S. Ramadan, G. Su, C. Huo, Y. Zhao, J. Liu, L. C. Hsieh-Wilson and X. Huang, *Angew. Chem., Int. Ed.*, 2023, **62**, e202211985.
10 (*a*) Y. Zhang, M. Yang, Z. H. Park, J. Singelyn, H. Ma, M. J. Sailor, E. Ruoslahti, M. Ozkan and C. Ozkan, *Small*, 2009, **5**(17), 1990–1996; (*b*) R. B. Selvi, S. Chatterjee, D. Jagadeesan, P. Chaturbedy, B. S. Sumar, M. Sswaramoorthy and T. K. Kundu, *J. Nanobiotechnol.*, 2012, **10**, 35.